Available online at www.sciencedirect.com
SCIENCE DIRECT®
Materials Chemistry and Physics 89 (2005) 249–252
MATERIALS CHEMISTRY AND PHYSICS
www.elsevier.com/locate/matchemphys

Growth and characteristics of near-stoichiometric Zn:$LiNbO_3$ crystals grown by TSSG method

Shuangquan Fang*, Biao Wang, Tao Zhang, Furi Ling, Yequan Zhao

Electro-Optics Technology Center, Harbin Institute of Technology, P. O. Box 1225, Harbin 150001, China

Received 16 February 2004; received in revised form 22 June 2004; accepted 28 June 2004

Abstract

A series of near-stoichiometric Zn:$LiNbO_3$ (Zn:NSLN) crystals were grown by the top seed solution growth (TSSG) method using K_2O as flux. Defect structures and Zn^{2+} occupation mechanism were analyzed and discussed by X-ray powder diffraction (XRD), differential thermal analysis (DTA), ultraviolet-visible (UV) absorption and infrared (IR) spectrum measurement. Moreover, we also found that the threshold concentration of ZnO in NSLN were between 2 and 3 mol%.

Keywords: $LiNbO_3$; Near-stoichiometric; Dsefect structure; Threshold

1. Introduction

$LiNbO_3$ (LN) single crystal belongs to trigonal crystal system, whose point group is 3 m in room temperature and space group is *R*3*C* [1]. For its excellent piezoelectric, electro-optic and nonlinear optic properties, the crystal is widely use in many fields, e.g. transducer, acoustic surface wave device, holographic memories. It is a well-known fact that all these properties are affected significantly by intrinsic and extrinsic defects due to the non-stoichiometry, impurities or dopants [2]. Protons, in the form of OH^- ions, are always present in air-grown $LiNbO_3$ though not intentionally doped [3]. It has been proved that OH^- ions play an important role in thermal fixation of holograms in $LiNbO_3$ [4]. In 1980, Zhong et al. [5] first reported that many properties exhibit abrupt changes when MgO dopant content reached a certain value, that is, so called "threshold concentration". Later, this phenomenon was also found in $LiNbO_3$ crystals doped with Zn, In or Sc [6–8]. Moreover, it has been demonstrated that control of non-stoichiometric defects in $LiNbO_3$ was of key importance for improving many physical and optical properties [9].

Many investigations have been carried out about the threshold concentration and defect structure in congruent $LiNbO_3$ (CLN) crystals doped with M (M = Mg, Zn, In or Sc) in recent years [5–8]. But the relation between the dopant and crystal properties is still unclear in near-stoichiometric $LiNbO_3$ (NSLN) crystals doped with M. In this work, we grew a series of NSLN crystals doped with Zn and studied their structure properties by X-ray powder diffraction, DTA, UV absorption and IR spectrum measurement.

2. Experimental procedure

2.1. Specimens preparation

All studied near-stoichiometric specimens had been grown in air atmosphere from congruent melts containing 10.7 mol% K_2O by the top seed solution growth (TSSG) method. All raw materials Li_2CO_3, Nb_2O_5, K_2CO_3 and ZnO were of 99.99% purity and were mixed for 24 h. ZnO contents in melt were 0–3 mol%, respectively. The mixtures were heated to 750 °C for 2 h to decompose the carbonate, then to

* Corresponding author. Tel.: +86 45186400661; fax: 86 45186400661.
E-mail addresses: shqfang@yahoo.com.cn, wangbiao@hit.edu.cn (S. Fang).

0254-0584/$ – see front matter © 2004 Elsevier B.V. All rights reserved.
doi:10.1016/j.matchemphys.2004.06.030

1050 °C for 2 h to prepare polycrystalline materials through the method of solid reaction. The temperature of solid reaction was cooled down for using K_2O as flux, which avoided raw materials melted locally. The crystals were grown using *c*-axis seed crystal from the polycrystalline materials in an intermediate frequency (IF) heater furnace. The crystals were grown at rotating rate 40 rpm and pulling rate 0.1 mm h^{-1}, and about 10% of the melt was crystallized. The crystals were annealed to room temperature in air at the speed of 40 h^{-1}.

It was found by HF–HNO_3 (1:2) etching experiments that all as-grown crystals had almost single-domain structure, therefore required no poling treatment, which avoided introducing cracks or scattering centers into the congruent crystals. In contrast to most other dopants nearly all potassium remains in the melt, which have been confirmed by an electron microprobe experiment [10], thus the influence of K on the crystal properties can be neglected. For spectrum measurements, the crystals were sliced into wafers perpendicular to the *y*-axis and polished to a mirror surface on both sides using SiC powders and diamond paste.

2.2. Measurement

The X-ray powder analysis using a D/max-γB style X-ray diffractometer with a revolving anode were performed for phase identification and lattice constants determination. The Curie temperature of the specimens were measured by a DTA technique using ZRY-2P style differential thermal analyzer, which were recorded while slowly heating the specimens at a rate of 1 °C min^{-1} from room temperature to about 1260° in air. Adopting CARYIE style UV–vis spectrophotometer, the absorption spectra of the crystals were measured in the 300–900 wavelength range, while the infrared absorption spectra of the crystals were measured by Flourier infrared spectrophotometer.

3. Results and discussions

X-ray powder analysis confirmed that all crystals were single phases of LN. The lattice constants of crystals were calculated by the least-squares method and listed in Table 1. The unit cell volumes were also given by the formula $V = (a^2c) \times \cos 30^\circ$. The variation of the lattice constants and the unit cell volume with the ZnO content in melt was shown in Fig. 1. It was clear that in the near-stoichiometric samples, both of lattice constants and their ratios (*c*/*a*) increased with ZnO content increasing, thus the unit cell volume of crystals also increased. From Table 1 and Fig. 1, we can assume that the crystal structure of NSLN was much closer to that of CLN with ZnO content increasing. Ionic radii of Zn ions (r_{Zn} = 0.74 Å) were much closer to that of Nb ions (r_{Nb} = 0.68 Å) than that of Li ions (r_{Li} = 0.60 Å), therefore Zn ions should prefer to replace Nb ions rather than Li ions.

Table 1
Lattice constants of congruent and Zn-doped near-stoichiometric crystal samples

No.	ZnO (mol%)	*a* (nm)	*c* (nm)	*c*/*a*	*V* (nm^3)
C	0	0.51487	1.38625	2.69243	0.31825
S0	0	0.51413	1.38170	2.68745	0.31629
S1	1	0.51448	1.38342	2.68897	0.31712
S2	2	0.51463	1.38397	2.68925	0.31743
S3	3	0.51478	1.38455	2.68960	0.31775

Where "C" denotes congruent sample, and "S" denotes the near-stoichiometric sample.

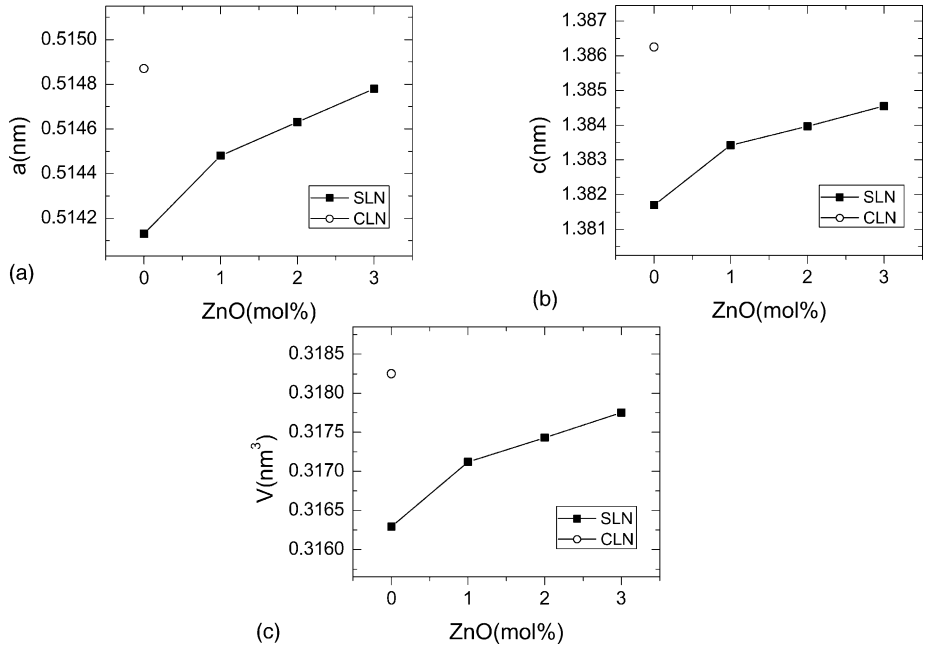

Fig. 1. Lattice constants and unit cell volumes as a function of ZnO content in melt according to Table 1.

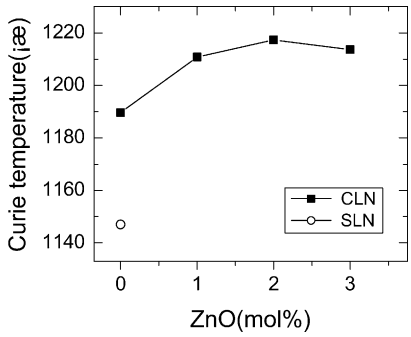

Fig. 2. Curie temperature as a function of ZnO content in melt.

In Fig. 2, the Curie temperature for NSLN was plotted as a function of ZnO content in the melt. In $LiNbO_3$ crystals, the Curie temperature reflected the Nb concentration of crystal, which increased with the decrease of Nb_{Li} (anti-site Nb, Nb in Li site) concentration or the increase of Nb_{Nb} (normal Nb site) [11]. On the basis of Li vacancy model [12], the formula of $LiNbO_3$ was expressed as $[Li_{1-5x}(V_{Li})_{4x}(Nb_{Li})_x]NbO_3$, where V_{Li} denoted as Li vacancy. In contrast with that of CLN, the Curie temperature of SLN increased for intrinsic defect Nb_{Li} concentration decreasing. From Fig. 2, the Curie temperature reached a maximum value when ZnO doped concentration was between 2 and 3 mol% in near-stoichiometric samples. At this doping level, all Nb_{Li} ions were completely replaced by Zn ions, and this doping level of ZnO was called as "threshold concentration". When ZnO dopant concentration was lower than "threshold", Nb_{Li} ions were gradually replaced by Zn ions, thus the Curie temperature will increase; otherwise, when ZnO dopant concentration was higher than "threshold", all Nb_{Li} ions were replaced and Zn ions began to occupied Li_{Li} site (normal Li site) and Nb_{Nb} site simultaneously, which made Nb_{Nb} ions decreased, so the Curie temperature will decrease.

We presented the absorption spectra of Zn:NSLN in Fig. 3. The absorption edge of Zn:NSLN crystals shifted to shortwave direction and the shift extent increased with the ZnO content increasing. Moreover, in contrast CLN samples, that of NSLN also exhibited a shift towards shortwave direction [13]. The basal absorption edge was decided by valence electron transition energy from valence band to conduction band. Band structure of $LiNbO_3$ was shown in Fig. 4, in which 2p orbits of O^{2-} acted as the top of valence band and 4d orbits of Nb^{5+} acted as the bottom of conduction band. In CLN sample, there existed a lot of anti-site defects, i.e. Nb_{Li}^{4+}, which acted as electron traps for positive charge. Therefore, these defects formed a localized state in the forbidden band and made forbidden band shallow. In NSLN samples, the forbidden band will be widen for anti-site defects, i.e. Nb_{Li}^{4+}, decreasing, so the energy for valence electron transition will increase, which resulted in blue-shift of absorption edge. In Zn:NSLN, Zn replaced Nb_{Li}^{4+} when Zn concentration was lower than "threshold", so Nb_{Li}^{4+} concentration decreased and Zn_{Li}^{+} generated, which will make forbidden band widen, too, thus absorption edge also exhibited blue-shift; otherwise, when doping Zn concentration higher than "threshold", all Nb_{Li}^{4+} were completed replaced and Zn ions began to replace Li_{Li} and Nb_{Nb} simultaneously, thus forming Zn_{Li}^{+}–Zn_{Nb}^{3-} charge self-compensating structure, which will make forbidden band more widen, therefore blue-shift extent of absorption edge increase further.

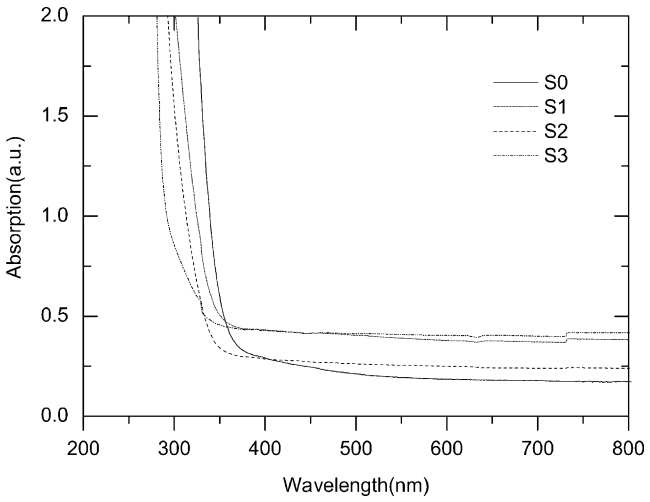

Fig. 3. UV absorption spectrum of Zn:NSLN.

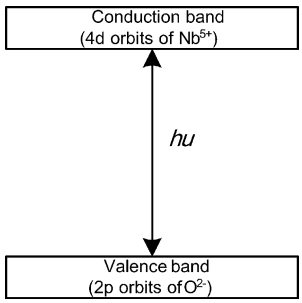

Fig. 4. Band structure of $LiNbO_3$.

The infrared absorption spectra measurement result was shown in Fig. 5. It can be seen from Fig. 5 that the OH^- absorption peak of samples S0, S1 and S2 located at 3466 cm^{-1} and that of S3 sample was at 3528 cm^{-1}, whereas that of CLN was at 3481 cm^{-1}. In $LiNbO_3$ crystals, H^+ was confirmed to occupied Li site, which had been reported by Kong et.al. [14] using ^1H nuclear magnetic resonance measurement. We thought that 3466 cm^{-1} absorption peak was responsible for the vibration of OH_{VLi}^- for H^+ locating at V_{Li} in S0 sample, i.e. pure NSLN, whereas that of 3481 cm^{-1} was caused by the vibration of OH_{Li}^- for H^+ replacing normal Li sites in CLN sample. In CLN sample, there were more anti-defects Nb_{Li}^{4+} than that in NSLN, therefore H^+ will be repelled to incorporate to Li site, not V_{Li} site, otherwise, H^+ will occupy V_{Li} site in NSLN crystals. In NSLN, OH_{VLi}^- being repelling intensively by Nb_{Li}^{4+}, fewer energy will be required for OH_{VLi}^- vibration than the case in CLN, so absorption peak exhibited red-shift in comparison with CLN. When Zn dopant con-

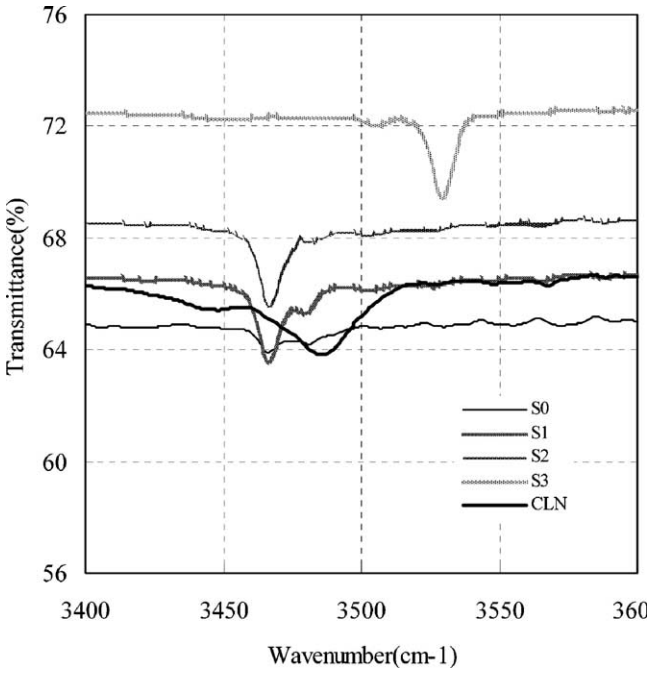

Fig. 5. IR transmittance spectra of Zn:NSLN and CLN.

centration in NSLN was lower than "threshold", Zn will replace $Nb_{Li}{}^{4+}$ to form $Zn_{Li}{}^{+}$, there will be not more H^+ in the vicinity of V_{Li} site for intensive repulsion, so absorption peak still located at 3466 cm^{-1} caused by $OH_{VLi}{}^{-}$ vibration. Otherwise, when Zn dopant concentration in NSLN was higher than "threshold", all $Nb_{Li}{}^{4+}$ was replaced completely and Zn began to enter into normal Li and Nb sites, forming $Zn_{Li}{}^{+}$–$Zn_{Nb}{}^{3-}$ charge self-compensating structure. Thus $Zn_{Li}{}^{+}$–$Zn_{Nb}{}^{3}$–OH^- defect structure formed for $Zn_{Nb}{}^{3-}$ had an intensive attraction for H^+, so more energy was required for OH^- vibration, which resulted in blue-shift of absorption peak, to 3528 cm^{-1}.

4. Conclusion

In conclusion, Zn:NSLN crystals were grown by the TSSG method. Measurement results showed that the threshold concentration of Zn:NSLN crystal was between 2 and 3 mol%. UV absorption edge of Zn:NSLN exhibited blue-shift with the Zn concentration increasing. In Zn:NSLN crystals, OH^- peak value located at 3466 cm^{-1} in the case of Zn concentration lower than threshold concentration, otherwise, OH^- peak shifted to 3528 cm^{-1}. Based on Li-vacancy model, we thought Zn^{2+} ions first replaced $Nb_{Li}{}^{4+}$ ions to form $Zn_{Li}{}^{+}$ ions, thus began to occupy normal Li and Nb site simultaneously and generated $Zn_{Li}{}^{+}$–$Zn_{Nb}{}^{3-}$ charge self-compensating structures.

Acknowledgement

This work was supported by the National Natural Science Foundation of China (50232030, 10172030), The National Science Foundation of Heilongjiang Province, The Ministry of Science and Technology of China through the High-Tech Program (2001AA31304), and the National Committee of Defense Science and Technology.

References

[1] O.F. Schirmer, O. Thiemann, M. Wöhlecke, J. Phys. Chem. Solids 52 (1991) 185.
[2] G. Zhang, Y. Tomita, X. Zhang, J. Xu, Appl. Phys. Lett. 81 (2002) 1393.
[3] Y. Kong, J. Xu, W. Zhang, G. Zhang, J. Phys. Chem. Solids 61 (2000) 1331.
[4] H. Vormann, G. Weber, S. Kapphan, E. Krätzig, Solid State Commun. 40 (1981) 543.
[5] G.G. Zhong, J. Jian, Z.K. Wu, Proceedings of the eleventh International Conference on Quantum Electronics, IEEE, New York, 1980, p. 631.
[6] T.R. Volk, V.I. Pryalkin, N.M. Rubinina, Opt. Lett. 15 (1990) 996.
[7] T.R. Volk, N.M. Rubinina, Ferroelectr. Lett. 14 (1992) 37.
[8] J.K. Yamamoto, K. Kitamura, N. Iyi, S. Kimura, Y. Furukawa, M. Sato, Appl. Phys. Lett. 61 (1992) 2156.
[9] X.-J. Chen, D.-S. Zhu, B. Li, T. Ling, Z.-K. Wu, Opt. Lett. 26 (2001) 998.
[10] G.I. Malovichko, V.G. Grachev, O.F. Schirmer, Solid State Commun. 89 (1994) 195.
[11] Y. Furukawa, K. Kitamura, S. Takekawa, K. Niwa, Y. Yajima, N. Iyi, I. Mnushkina, P. Guggenheim, J.M. Martin, J. Cryst. Growth 211 (2000) 230.
[12] P. Lerner, C. Legras, J.P. Dumas, J. Cryst. Growth 3–4 (1968) 231.
[13] G.I. Malovichko, V.G. Grachev, E.P. Kokanyan, O.F. Schirmer, K. Betzler, B. Gather, F. Jermann, S. Klauer, U. Schlarb, M. Wöhlecke, Appl. Phys. A 56 (1993) 103.
[14] Y. Kong, J. Xu, W. Zhang, G. Zhang, J. Phys. Chem. Solids 61 (2000) 1331.